

Chapter 19: Human tongue biomechanical modeling

N. Hermant^{1,2,3}, P. Perrier² & Y. Payan¹

1 Univ. Grenoble Alpes & CNRS, TIMC-IMAG, F-38000 Grenoble, France, yohan.payan@univ-grenoble-alpes.fr;

2 Univ. Grenoble Alpes & CNRS, Gipsa-Lab, F-38000 Grenoble, France, pascal.perrier@gipsa-lab.grenoble-inp.fr;

3 Universidad del Valle, School of Mechanical Engineering, Cali, Colombia, nicolas.hermant@correounivalle.edu.co

Abstract:

This chapter introduces the anatomy of the human tongue, with its complex interweaving of muscles, glands and connective tissues, which shape is determined by the recruitment of ten muscles or so, some of them being internal to the structure. The most known constitutive models proposed in the literature to describe the complex mechanical behaviors of tongue tissues are introduced and discussed. These models assume a hyperelastic material modeled using a strain energy approach.

A Finite Element implementation of an incompressible two-parameter Yeoh strain energy was proposed to simulate tongue tissues deformations in response to muscle activations. Such constitutive model was estimated from an indentation experiment done on the fresh cadaver of a 74-year old woman. Simulated tongue deformations under muscle activations were then provided. It is shown that the very soft material chosen to account for tongue tissues elasticity allows simulating the very large strain values observed inside the tongue tissues with tagged MRI, while maintaining a level of stress in tongue muscles coherent with data provided in the literature. Such results show the importance of the choice for a constitutive law when the organ model is driven by muscles forces.

Keywords: Tongue tissues, Finite Element modeling, constitutive material model, large deformations.

1. Introduction: human tongue anatomy

Tongue is crucial for the achievement of basic biological functions in humans, such as licking, swallowing and speaking. It is a muscular hydrostat that fills almost the entire oral cavity. It is rooted in the pharyngeal cavity just above the larynx and it develops towards the front up to the teeth. Depending on the sex and the size of the subject, the tongue volume varies between 60 and 80 cm³, for a length of about 10cm and a maximal width of 5cm. Tongue tissues' density is close to 1, which makes that tongue weight varies in the range of 60 to 80g. Details about tongue anatomy can be found in particular in Zemlin (1968), Miyawaki (1974), Khane & Folkins (1984) and Takemoto (2001). The main features are summarized below.

In its low and posterior part, called "tongue root", the tongue is attached to the hyoid bone, a small U-shaped mobile bone located at rest just above the thyroid cartilage, below the mandible, at the height of the third cervical vertebrae (Boë et al., 2013). Contrary to all the other bones of the human skeleton, the hyoid bone is not articulated with another bone. It is free to move under the activation of 7 muscles pairs that connect it on both sides of the head to the mandible (mylohyoid and geniohyoid muscles, and anterior belly of the digastric muscle), the skull (the mastoid process via the posterior belly of the

digastrics muscle, and the styloid process via the stylohyoid muscle), sternum (sternohyoid muscle), the shoulder (omohyoid muscle) and the thyroid cartilage (thyrohyoid muscle). The movements of the hyoid bone influence the position of the tongue root.

In its low and anterior part the tongue is connected to the mandible, just behind the chin, in the mental spine. Between the hyoid bone and the mental spine, the tongue body lies just above the mylohyoid and geniohyoid muscles, building what it classically called the “mouth floor”. Thus, the mandible and the mouth floor sustain the tongue, and their vertical displacements largely influence the vertical position of the tongue and its proximity to the palate.

As any muscular hydrostat, the tongue is essentially made of muscles that, in combination with the jaw and hyoid bone movements, will determine its shape and, in case of contacts with external structures such as the palate or the teeth, the level of mechanical pressure in the contact region. The anterior part of the tongue, called *tongue tip*, is quite thin and very mobile. The tongue tip is connected to the anterior part of the mouth floor by a thin fibrous ligament, called *lingual frenulum*, which limits its elevation within a certain range. A thin fibrous membrane called *lingual septum* divides the tongue in two parts, approximately symmetrical, from either side of the midsagittal plane of the head. This is why all the muscles of the tongue are muscle pairs, except one, the *superior longitudinalis*, that lies above the upper extremity of the septum (see below). Tongue muscles are distributed across two main categories: the *extrinsic* muscles, on the one hand, which insert in the tongue at one extremity and on the jaw, the hyoid bone or the skull at the other extremity; the *intrinsic* muscles, on the other hand, which insert at both extremities in the tongue. The extrinsic muscles are the *Genioglossus*, the *Hyoglossus*, the *Styloglossus* and the *Palatoglossus*. The intrinsic muscles are the *Superior Longitudinalis*, the *Inferior Longitudinalis*, the *Verticalis* and the *Transversalis*.

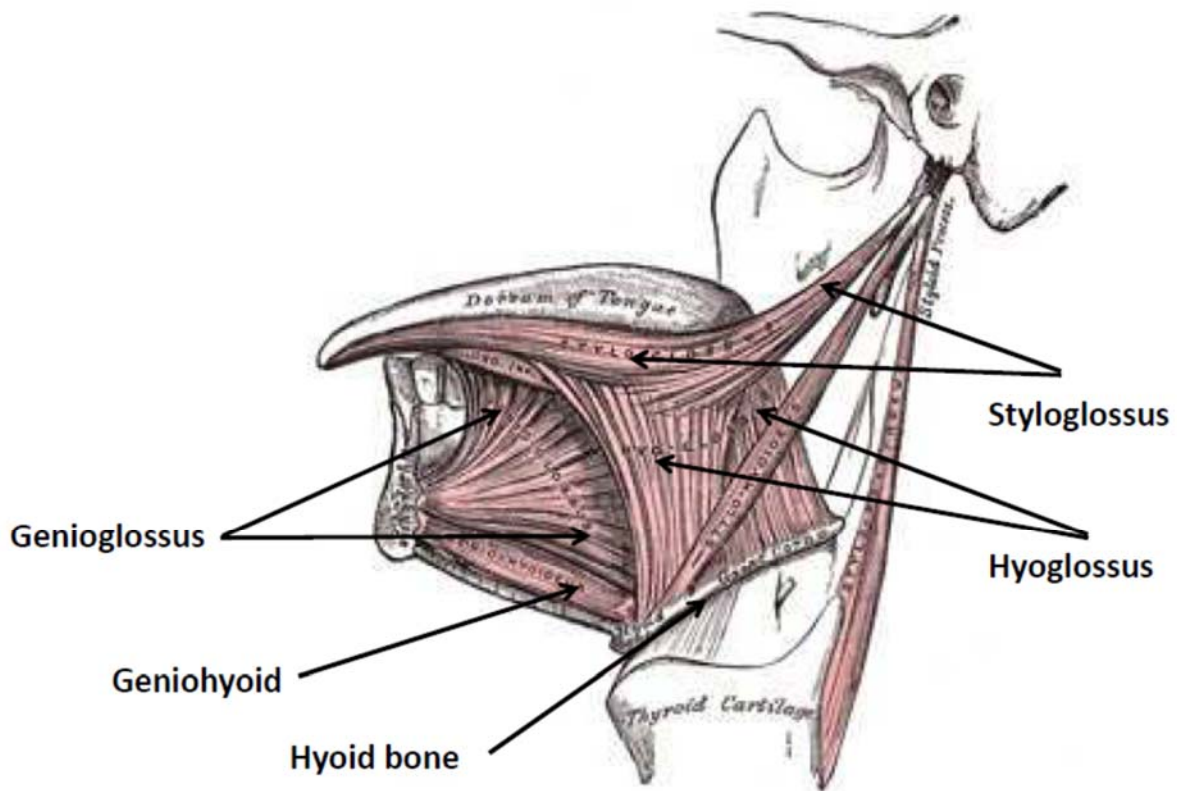


Figure 1: Side view of the tongue showing the three main extrinsic muscles of the tongue. Front is on the left. For clarity reasons, the Geniohyoid muscle that connects the hyoid bone and the jaw is also indicated (adapted from Gray, 1918 in Bartleby.com, 2000).

The *Genioglossus* is the largest and thickest muscle of the tongue. Its volume represents a large part of the volume of the tongue. It has the shape of a fan, parallel to the midsagittal plane of the head, starting from the mental spine and developing backwards and upwards over a large domain going from the hyoid bone to the posterior part of the tongue tip. Thus, its lowest fibers run from the front to the back parallel to the mouth floor and inserts on the hyoid bone, while its most anterior fibers run almost vertically toward the upper part of the tongue (Figure 1). It is located in the middle of the tongue and surrounds the lingual septum (Figure 2). Functionally, it is now usual to consider that the *Genioglossus* is divided in three different parts, from the back to the front. The *Posterior Genioglossus* goes from the mental spine toward the internal surface of the Superior Longitudinalis (see below) and spreads over roughly the whole vertical part of the tongue in the pharynx. Its activation moves the tongue root forward toward the mental spine, and compresses the lowest part of the tongue. Due to the hydrostatic properties of the tongue, this compression generates an elevation and a forward movement of the upper part of the tongue located in the palatal region of the oral cavity. The *Medium Genioglossus* goes from the mental spine to the part of the tongue located in the velar region of the vocal tract below the internal surface of the Superior Longitudinalis. Its activation flattens the tongue in this region and generates a forward, possibly slightly upward, movement of the tongue tip. The activation of the remaining part of the *Genioglossus*, called *Anterior Genioglossus*, lowers the tongue blade in the front part of the palatal region of the oral cavity, and may generate a slight backward movement of the tongue in the pharynx.

The fibers of the *Styloglossus* run from the styloid process located on both sides of the skull, below the ear, in the front part of the temporal bone, toward the sides of the tongue in the upper part of the pharynx (Figure 2). Once the fibers coming from the styloid process have reached the tongue, they spread on each side of the tongue into two different bundles (Saito & Itoh, 2007). The first bundle goes further forward on the side of the tongue, and inserts in the lower part of the tongue tip (Figure 1). The second bundle penetrates into the tongue and inserts in the lingual septum, making thus an arch crossing the midsagittal plane of the head. The activation of the *styloglossus* generates an elevation of the tongue in the palatal and velo-palatal region, and a lowering of the tongue tip. It is also generally assumed to pull the body of the tongue backwards, but this assumption has recently been contested on the basis of MRI data recorded from a Japanese speaker during vowel production (Takano & Honda, 2007).

The *Hyoglossus* has the shape of a rectangle located on both sides of the tongue. Its fibers insert, in the back, on the great horns of the hyoid bone (Figure 1), and from there they run upward, and slightly forward, up to the sides of tongue body, just in front of the location where the fibers of the *Styloglossus* penetrate into the tongue (Figure 2). The activation of the *hyoglossus* generates a lowering of the tongue and pulls it backward.

The *Palatoglossus* is the smallest extrinsic muscle of the tongue. It runs from the lateral parts of the soft palate toward the sides of the tongue in the upper part of the velo-pharynx. Its activation brings the velum and the tongue closer, essentially by moving the velum downward.

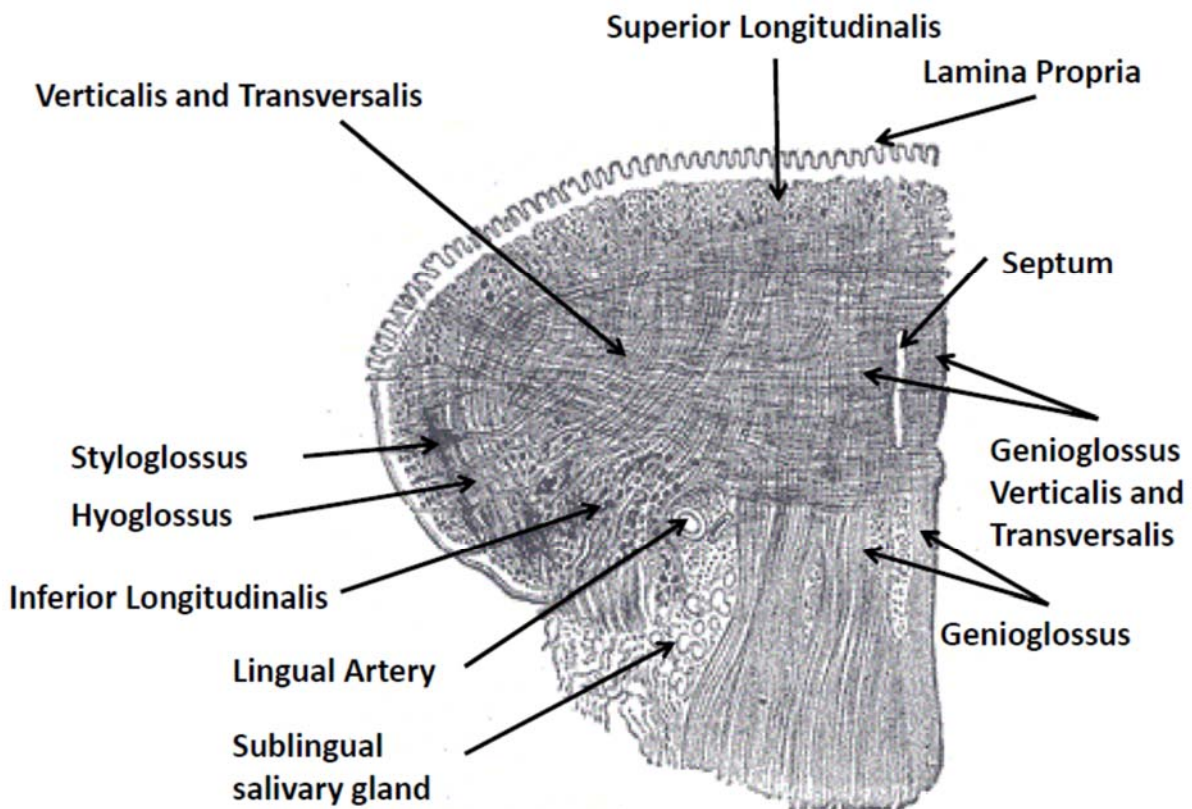


Figure 2: Partial coronal cut of the tongue in the region of the soft palate showing the anatomical implementation of the main extrinsic and intrinsic muscles of the tongue. The center of the tongue along the right-to-left direction is marked by the septum. Only one side of the tongue and a small part of the other side are shown (adapted from Gray, 1918 in Bartleby.com, 2000).

The fibers of the *Superior Longitudinalis* run longitudinally along the surface of the tongue from the tongue tip to the tongue root close to the hyoid bone. They cover the whole superior part of the tongue and are located just below the superficial mucosa, called *lamina propria* (Figure 2). In the front, according to Barnwell et al. (1978), the fibers run around the tongue tip and are connected to the lingual septum below it. The activation of the *Superior Longitudinalis* shortens the tongue along the front/back direction, retracts the whole tongue body toward the hyoid bone and can also generate an elevation of the tongue tip toward the alveolar part of the palate.

The *Inferior Longitudinalis* is a thin muscle, which fibers run on both sides of the tongue along the external boundaries of the *genioglossus* (Figure 2) from the lower part of the tongue tip toward the tongue root, just above the hyoid bone. Its activation lowers the tongue tip and shortens the tongue along the front/back direction.

The *Verticalis* and *Transversalis* muscles are essentially located in the same part of the tongue, just below the *Superior Longitudinalis*. They take up the majority of the tongue volume in this region over a height of about 2cm (Figure 2), from the tongue tip in the front toward the tongue root in the back (Takemoto, 2001). The fibers of the *Verticalis* run vertically, while those of the *Transversalis* run from the septum to the right and to the left part of the tongue. In the center of the tongue, around the septum, their fibers are intertwined with those of the *genioglossus* (Figure 2). The activation of the *Verticalis* compresses the tongue vertically, while the *Transversalis* controls the width of the tongue along the right/left direction.

The tongue movements are constrained by the walls of the oral cavity with which it is in frequent mechanical interaction through contacts. Upper walls of the oral cavity are in the back the soft palate, and in the front the lower part of the maxillary bone (hard palate and maxillary arch) and the upper teeth. Lower walls of the oral cavity are the upper part of the body of the mandible (the mandibular alveolar process and the mandibular arch) and the lower teeth. In the mouth floor, just above the mylohyoid, the space existing in the front between the genioglossus and the mandibular alveolar process is filled by the sublingual salivary gland (see Figure 2), and in the back the space existing between the hyoglossus and the mandibular alveolar process is filled by the submandibular salivary gland. In the back of the vocal tract walls are made of the inner parts of the superior and middle pharyngeal constrictors, two muscles that can also be activated to narrow the cross-section of the pharynx.

2. Tongue biomechanical modeling: a review of the constitutive models proposed in the literature

The muscular and connective tissues that constitute human tongue are complex materials that can exhibit non-linear, time dependent, inhomogeneous and anisotropic behaviors. Various constitutive models for describing such tissues have been proposed in the literature. Most of them assume a hyperelastic material modeled by using a strain energy approach (Wilhelms-Tricarico, 1995 ; Rodrigues et al., 2001 ; Gerard et al., 2003, 2005 ; Buchaillard et al., 2007, 2009 ; Stavness et al., 2012 ; Pelteret and Reddy, 2012 ; Wang et al., 2013). However, very few of them propose a constitutive model based on real data, because of the difficulty to perform experiments to measure the mechanical response of tongue tissues under physiological loading conditions. When such data are available, hypotheses about the constitutive model are formulated and the values of the corresponding constitutive parameters are estimated to make the model consistent with measurements. To our knowledge, only three papers have addressed this question with experimental data, and experiments were conducted *ex vivo* (Gerard et al., 2005) or *in vivo* (Schiavone et al., 2008 ; Cheng et al., 2011).

Gerard and colleagues (2005) carried out an indentation experiment by measuring the mechanical response of tongue tissues removed from the fresh cadaver of a 74-year old woman (Figure 3, top panel). Non-linear relationships were observed between the force applied to the tissues and the corresponding displacements. To infer a constitutive model from these measurements, a finite element (FE) analysis of the indentation experiment was provided (figure 3, low panel), assuming the constitutive model to be an incompressible two-parameter Yeoh strain energy. An optimization process was used to determine the parameters of the Yeoh material that provided non-linear force/displacements matching those observed during the indentation experiments. Values of 192Pa and 90Pa were respectively estimated for the C_{10} and C_{20} parameters of the Yeoh strain energy function W given in Equation (1) (I_1 being the first invariant of the right Cauchy-Green strain tensor):

$$W = C_{10} (I_1 - 3) + C_{20} (I_1 - 3)^2 \quad (1)$$

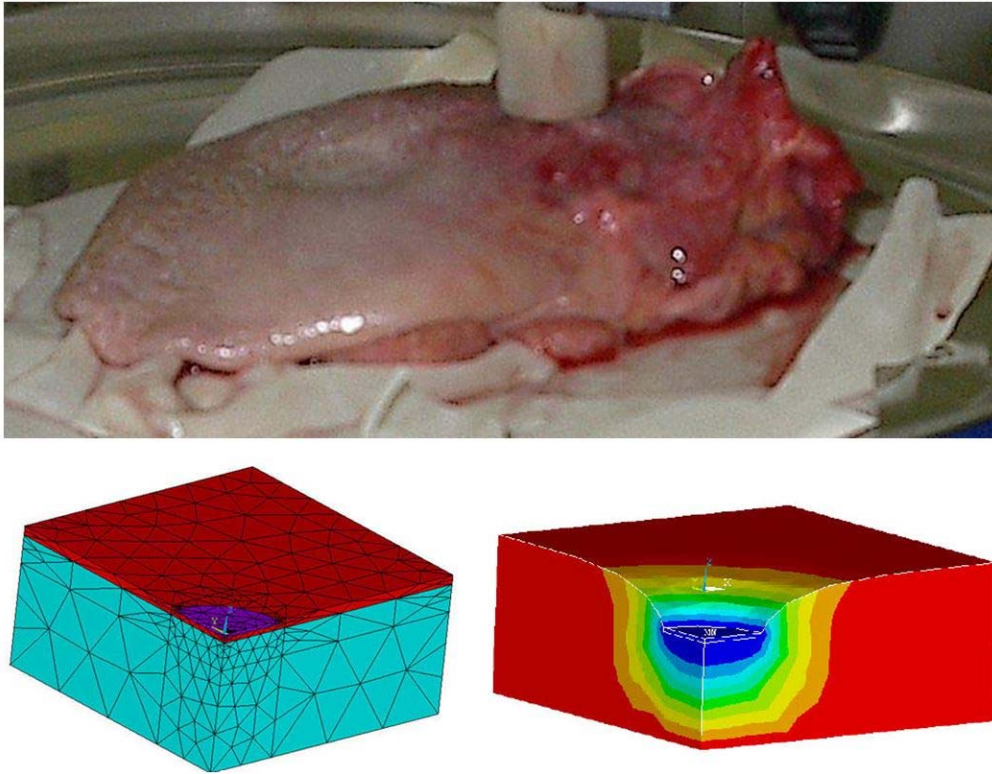


Figure 3: Ex vivo tongue indentation (top panel) and the corresponding FE analysis (low panel; mesh modeling the piece of tissue on the left; mechanical stress induced at rest on the piece of tissue, on the right)

More recently, *in vivo* experiments were conducted to estimate tongue constitutive models. Indeed, it has clearly been shown (Kerdok et al., 2006; Ottensmeyer, 2002; Gefen and Margulies, 2004) that the mechanical behavior of soft tissue can differ significantly between *in vivo* and *ex vivo* conditions, for a number of reasons, including the vascularization of the tissue and the fact that some *ex vivo* tissues were not extracted from a fresh cadaver.

Using a light aspiration device for which the deformation of the aspirated tissue is imaged via a mirror using an external camera, Schiavone and colleagues (2008) provided an estimation of the *in vivo* tongue constitutive behavior (figure 4). The subject was asked to put his tongue in two configurations: first, in a rest position with the objective to measure the “passive” component of the tongue constitutive material, and second in a stiffened condition, with the objective to estimate tongue stiffening due to muscles activations.



Figure 4: In vivo tongue aspiration

An FE analysis of the aspiration experiment was proposed, assuming again the constitutive law of the material to be an incompressible two-parameter Yeoh strain energy function. An optimization algorithm, fitting the measured tongue deformation inside the aspiration device, provided estimations of the C_{10} and C_{30} parameters of the Yeoh strain energy function W :

$$W = C_{10} (I_1 - 3) + C_{30} (I_1 - 3)^3$$

Values of 700Pa and 3050Pa were obtained for respectively estimating the C_{10} and C_{30} parameters when tongue is at rest. It is interesting to note that a ratio in the order of 3.5 is observed for C_{10} between the value estimated from experiments conducted *ex vivo* ($C_{10} = 192\text{Pa}$, Gerard et al., 2005) and the *in vivo* value ($C_{10} = 700\text{Pa}$, Schiavone et al., 2008). This ratio is probably due to muscle tone that is present even if the subject was asked to not activate his tongue muscles. When the subject was asked to “*make his tongue active*”, it is interesting to note that a much higher value was estimated for C_{10} ($C_{10} = 4440\text{Pa}$).

Finally, Cheng and colleagues (2011) investigated the *in-vivo* viscoelastic properties of the tongue using Magnetic Resonance Elastography (MRE). During quiet breathing, seven healthy volunteers were requested “*to keep still and rest their tongue on the hard palate close to the upper teeth during the scans*” (Cheng et al., 2011, p. 451). Results show a mean shear modulus μ value of 2670Pa, which is coherent with values estimated by Gerard et al. (2005) and Schiavone et al. (2008). Indeed, as shown in table 1 (knowing that $\mu = 2 C_{10}$), the shear modulus value estimated with this MRE exam is higher than the one estimated *ex vivo* by Gerard et al. (2005). Moreover, the value is also higher than the one estimated *in vivo* by Schiavone et al. (2008), which was expected since keeping the tongue in

contact with the palate, as compared to the tongue rest position, needs additional muscle activations that stiffen the tissues (and therefore provide a shear modulus larger than the one observed when only muscle tone is present). However, the 2670Pa value estimated here is still lower than the 8880Pa value provided by Schiavone et al. (2008) for measurements with an explicit request to “activate tongue muscles”.

Reference	Tongue shear modulus μ (Pa)	Experimental conditions
Gerard et al. (2005)	384	ex vivo indentation (fresh cadaver)
Schiavone et al. (2008)	1400	in vivo aspiration (tongue at rest)
Schiavone et al. (2008)	8880	in vivo aspiration (tongue “active”)
Cheng et al. (2011)	2670	in vivo MRE (tongue against the palate)

Table 1: Summary of the mechanical properties (shear modulus) of the tongue measured using different techniques

Before introducing the 3D FE model of the tongue that was developed in our group and based on our *ex vivo* and *in vivo* measurements (respectively Gerard et al., 2005 and Schiavone et al., 2008), it is important to acknowledge other biomechanical tongue models proposed in the literature. We decided here to focus on 3D models that were assuming a hyperelastic modeling of tongue constitutive law. Table 2 lists these models from the earlier to the most recent one, indicating the choice for the constitutive model with the values of the corresponding parameters. Most models consider tongue tissues as a quasi-incompressible material (which means a large bulk modulus value or a Poisson ratio close to 0.5).

Reference	Constitutive model	Values / Comments
Wilhelms-Tricarico (1995)	$W = c_0 \left\{ \exp \left[c_1 (I_1 - 3)^2 + c_2 (-2I_1 + I_2 + 3) \right] - 1 \right\}$	Strain energy initially proposed for cardiac tissue. $c_0=0.5\text{kPa}$; $c_1=0.75$; $c_2=1.5$.
Rodrigues et al. (2001)	Mooney-Rivlin formulation	“Stiffness value close to 500kPa”
Gerard et al. (2003)	Five-parameter Mooney-Rivlin constitutive equation	$C_{10}=4.3\text{kPa}$; $C_{01}=-1.9\text{kPa}$; $C_{20}=2.1\text{kPa}$; $C_{11}=-1.8\text{kPa}$; $C_{02}=0.5\text{kPa}$
Gerard et al. (2005)	$W = C_{10} (I_1 - 3) + C_{20} (I_1 - 3)^2$	$C_{10}=192\text{Pa}$; $C_{20}=90\text{Pa}$
Buchailard et al. (2007 and 2009)	$W = C_{10} (I_1 - 3) + C_{20} (I_1 - 3)^2$	$C_{10}=1037\text{Pa}$; $C_{20}=486\text{Pa}$; values from Gerard et al. (2005) have been increased to account for muscle tone.
Mijailovich et al. (2010)	linear elastic elements for connective tissues + nonlinear skeletal muscle activation	Young’s modulus of 250kPa Hill-type muscle model

Stavness et al. (2012)	$W = C_{10} (I_1 - 3) + C_{20} (I_1 - 3)^2$	Same as Buchaillard et al. (2007 and 2009)
Pelteret and Reddy (2012)	$W = c(\exp[b(I_1 - 3)] - 1)$	$c = 2500\text{Pa}$; $b = 2.75$ for adipose tissues $c = 1652\text{Pa}$; $b = 0.62$ for muscle tissues
Wang et al. (2013)	Two-parameter Mooney-Rivlin constitutive equation	$C_1 = 375\text{Pa}$; $C_2 = 175\text{Pa}$
Yang et al. (2013)	Co-rotational modal warping (Choi, 2005)	Young's modulus of 6912Pa
Wu et al. (2014)	linear elastic elements for connective tissues + nonlinear muscle model	Young's modulus of 20kPa Extended Hill-type muscle model

Table 2: Summary of the 3D FE tongue hyperelastic models published in the literature

3. A 3D Finite Element model of the human tongue

Our currently used tongue model derives from the models developed by Gérard and colleagues (Gerard et al., 2003 & 2005) and Buchaillard and colleagues (Buchaillard et al., 2007 & 2009). It has been adapted and improved through the works of Rohan and colleagues (Rohan et al., 2016). The 3D geometry of this model is based on medical images of a specific subject (PB).

3.1. Geometrical structures and mesh creation

Mesh: The Bolt meshing software¹ was used to create a full hexahedral mesh from the 3D external surface of the tongue reconstructed from a manual segmentation of the MRI and CT images of PB. The mesh that has been used in the design of the 3D finite-element model of the human tongue described in this chapter is composed of 6534 hexahedral elements based on 8679 nodes. It is symmetrical with respect to the mid-sagittal plane.

Implementation of muscle anatomy: The starting point of the implementation of muscle anatomy in the mesh consists in the specification for each muscle of a region in the mesh, in which active force will be generated when the muscle is active. Within each of these regions, force is applied along directions locally specified by the local orientation of the muscle fibers. This work was done for the model used in this paper on the basis of our former work on the preceding version of the tongue model (Buchaillard et al., 2009), which was inspired by classical anatomy knowledge (Zemlin, 1968 ; Miyawaki, 1974 ; Khane & Folkins, 1984 ; Takemoto, 2001). Some regions of the tongue are associated with more than a muscle.

3.2. Mechanical properties and muscle activation model

Nazari and colleagues (Nazari et al., 2011 & 2013) have designed an active 3D muscle element suited to the finite element method. This model accounts for the passive elastic properties and the active force generation mechanisms of a muscle, by describing an active element as a volume in which muscle fibers are embedded in a matrix of surrounding passive tissues. Muscle force generation principles are modeled using either a Hill-type model of activation, based on Blemker et al. (Blemker

1 <http://www.csimsoft.com/boltoverview>

et al., 2005) formulation, or an original account of the λ -model proposed by Feldman (1986). For the simulations presented in this paper, Nazari et al.'s (2013) Hill-type muscle element has been used.

Thus, a muscle is modeled as a transversely isotropic material, with an isotropic passive behavior in the directions orthogonal to the muscle fibers and the combination of this passive behavior and an active behavior along the direction of the fibers. As a consequence, the mechanical properties are different in the direction of the muscle fibers and in the direction orthogonal to them.

In agreement with some of the previous approaches described in Sec. 2 of this chapter, the surrounding passive tissues are modeled using element material properties which follow a Mooney-Rivlin hyperelastic law. A simplified version of the strain-energy function W is used with only two constants, C_{10} and C_{20} , that are different from zero (Gerard et al., 2005; Buchaillard et al., 2009). For the simulations, the values proposed by Gerard et al. (2005), $C_{10}=192\text{Pa}$ and $C_{20}=90\text{Pa}$, have been used. The density of the tongue tissues has been set to 1040 kg/m^3 .

According to Hill-type models, the force along the muscle fiber direction can be modeled as the sum of the force generated by the passive tissues and the active force due to a contractile element. The contractile element generates force that is a time function of the muscle length and its derivative. The force-muscle length relation has been originally defined for a maximum voluntary force level (Hill, 1938 ; McMahon, 1984 ; Zajac, 1989). In Nazari et al.'s (2013) model, the activation level is tuned by multiplying the original force-muscle length curve by an activation parameter smaller than one. The force-velocity relation is modeled by multiplying the force-length relation with a factor smaller than one accounting for the decrease of the force with the rate of muscle length change, according to the sliding filament theory proposed by Huxley (1957). Doing so, the contractile element is assumed to act like a nonlinear spring whose stiffness varies depending on muscle activation, rate of muscle length change, and time.

3.3. Dynamic parameters and resolution method

The simulations, which results are presented in the next subsection, have been achieved activating independently each of the eleven muscles represented in Figure 5. Muscle activation has been set to last 500 ms, using a 0.1 activation factor. The effect of gravity has not been modeled.

The root of the tongue inserts in its back region on the hyoid bone (see above), which is mobile. In order to limit the complexity of the description proposed in this chapter, the mobility of the hyoid bone has not been modeled. Similarly, the mobility of the mandible that carries the tongue and influences its shape has not been modeled. Thus, a no-displacement constraint boundary condition has been used to constrain the tongue on its inferior base in its back, on the hyoid bone, as well as in its front on its insertion on the mandible. The contacts with the mandible are managed through an augmented Lagrangian method, which corresponds to an iterative series of penalty methods (Simo & Taylor, 1982)

For each muscle, the dynamic transient problem was solved using the ANSYSTM finite element software package, based on a full Newton-Raphson scheme. A Rayleigh damping model ($\alpha=20\text{s}^{-1}$ and $\beta=0\text{s}$) has been used (Bathe, 1982).

3.4. Muscle activation: simulations results

Figure 6 illustrates tongue deformations simulated from individual muscle activations starting from rest positions. Activation durations have been adjusted so as to generate strain amplitudes that are in agreement with experimental data.

The deformations are similar to those observed in former modeling studies (Wilhelms-Tricarico, 1995 ; Dang & Honda, 2004 ; Gerard et al., 2006 ; Fujita et al., 2007 ; Buchaillard et al., 2009 ; Pelteret & Reddy, 2012; Wu et al., 2014):

The posterior part of the genioglossus generates a global forward movement of the tongue body and an elevation in its anterior part. The medium and the anterior parts of the genioglossus lower respectively the mid-part and the anterior part of the tongue around the midsagittal plane, generating thus a grooving of the tongue in its dorso-alveolar region. The verticalis generates a slight downward

movement of the anterior part of the tongue associated with a grooving in the posterior part. The transversalis controls the tongue width in the transverse direction: its activation shrinks the tongue transversally in its palatal region and generates a slight forward movement of the tongue tip. The activation of the superior longitudinalis principally generates an elevation of the tongue tip, while an activation of the inferior longitudinalis results in a lowering and a backward movement of the tongue tip. The styloglossus elevates the tongue in its palatal part (dorsum) and pulls the tongue body backwards. The hyoglossus pulls the tongue backward and downward, narrowing the pharyngeal region. The hyoglossus pulls the tongue backward and downward, narrowing the pharyngeal region.

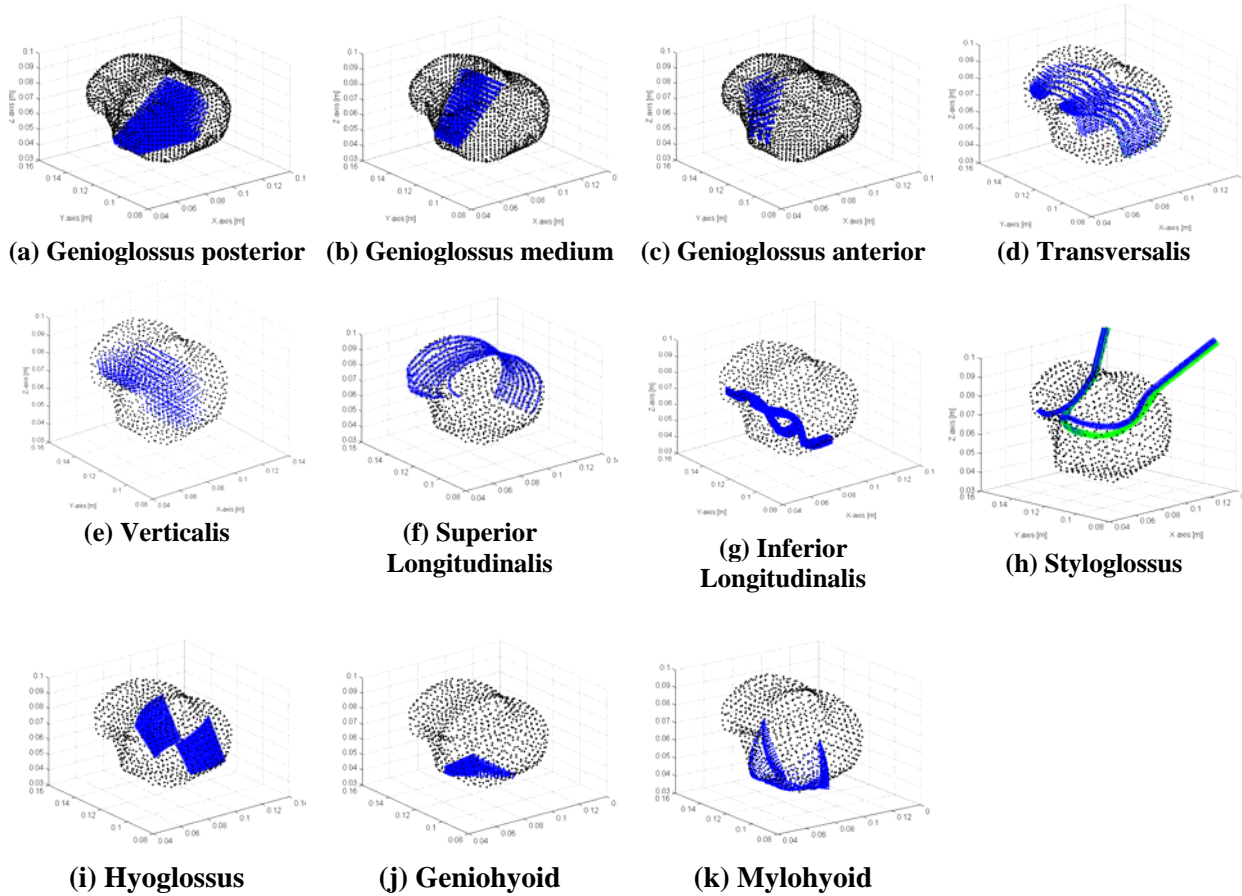


Figure 5: Definition of fiber paths (blue nodes) within the tongue mesh (black nodes)

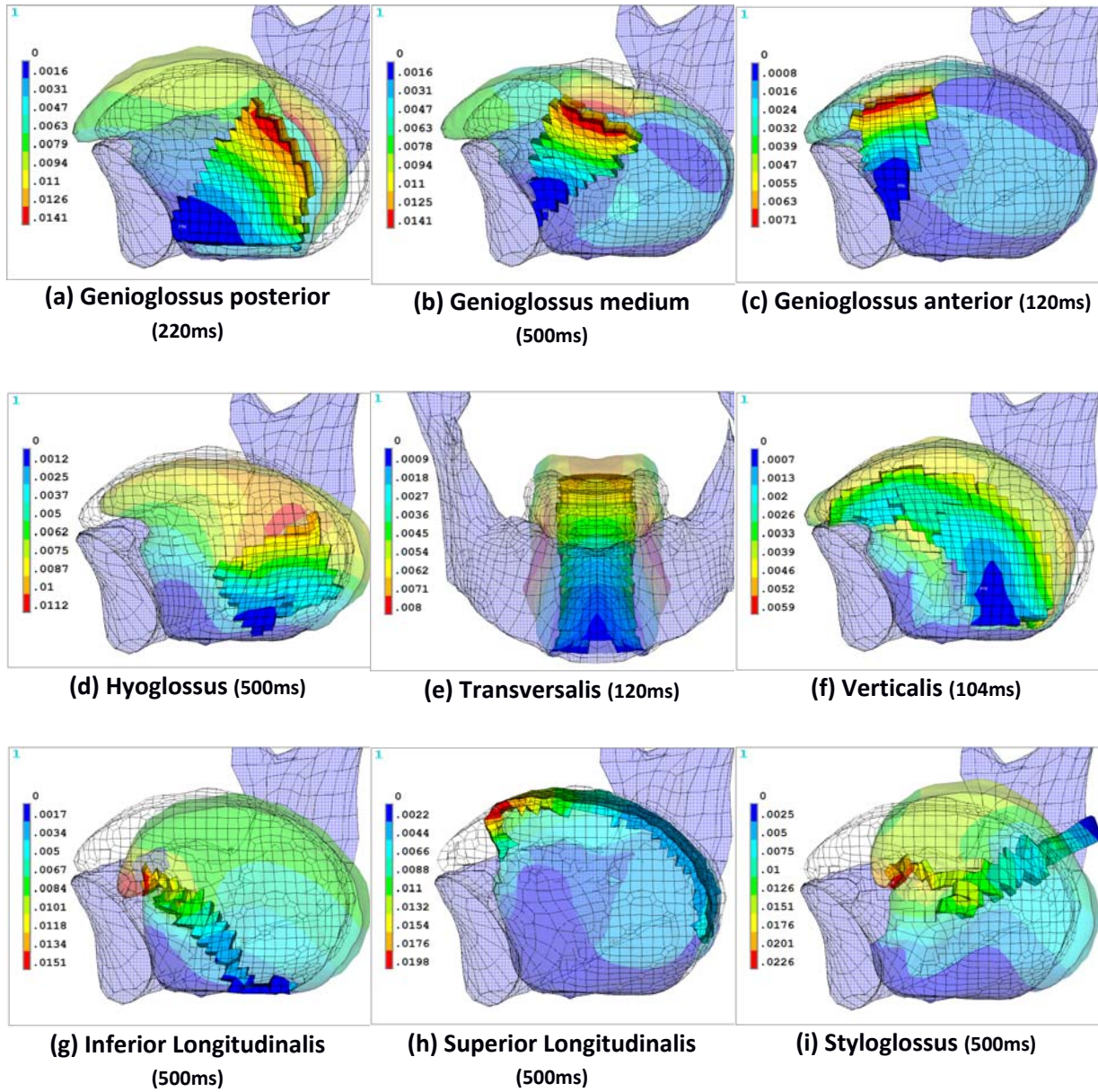


Figure 6: Sagittal cut (except for (e): front view) of mandible and tongue deformed shapes due to individual muscle activations (with suitable activation durations – see text). The color scale is used to show the nodal displacements (in mm). Each muscle is depicted as fully opaque, while the remaining parts of the tongue are partially transparent.

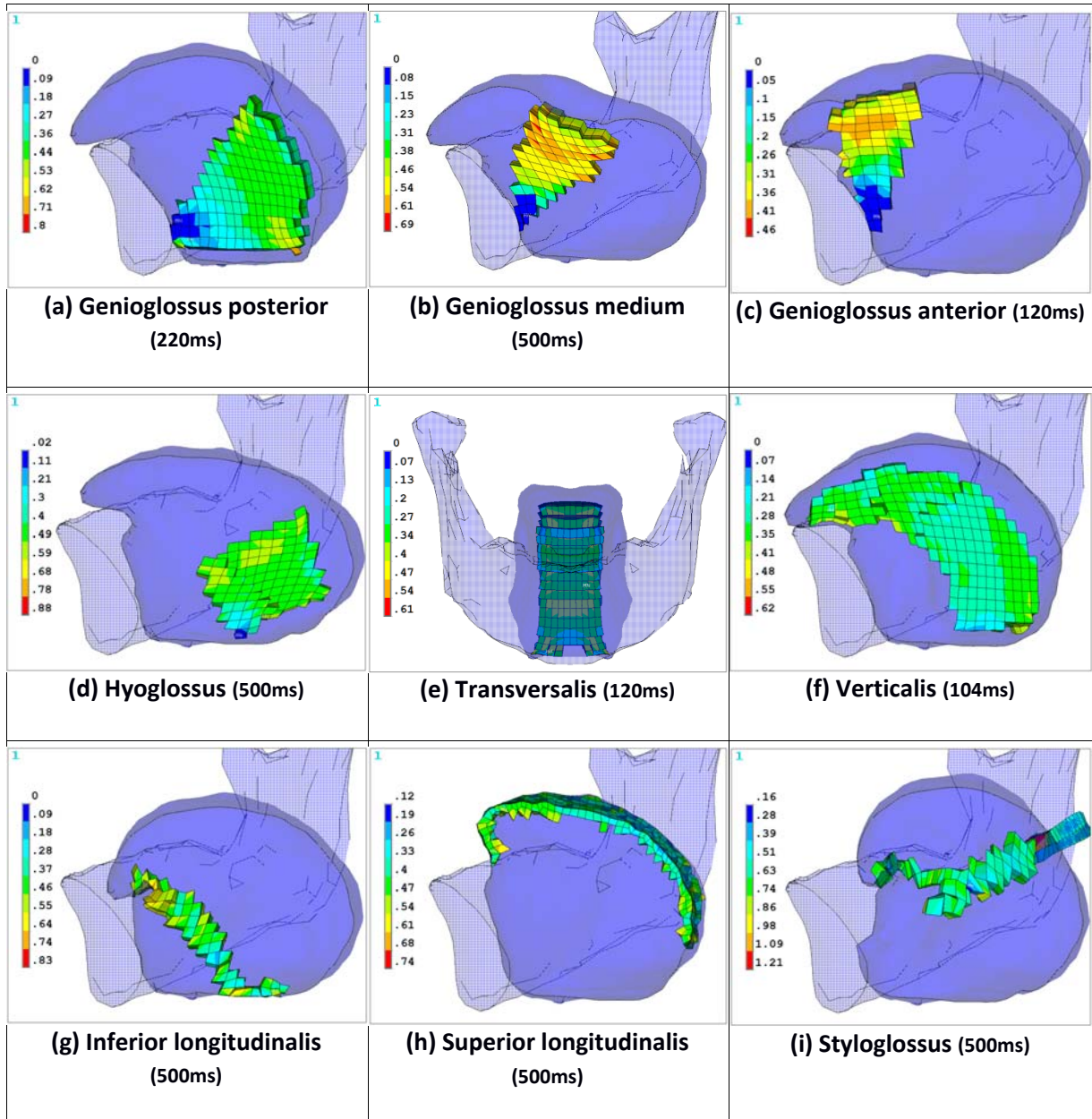


Figure 7: Sagittal cut (except for (e): front view) of mandible and tongue deformed shapes due to individual muscle activations (with suitable activation durations – see text). The color scale is used to show the Von Mises Strain values. Each muscle is depicted as fully opaque, while the remaining parts of the tongue are partially transparent.

Figure 7 plots the Von Mises strains values computed in each activated muscle. The interesting point illustrated here is the fact that the large deformation framework is clearly justified since maximal strain values in the range of 50 through 120% are observed across the muscles, The 120% value computed under the activation of the Styloglossus muscle could be considered as surprisingly high since most strain values usually observed in the literature for human soft tissues stay below 50%. However, as was reported by Napadow and colleagues (1999) from tagged MRI data, tongue is a very specific organ since strain values can reach 160% for tissues contraction and 200% in elongation,

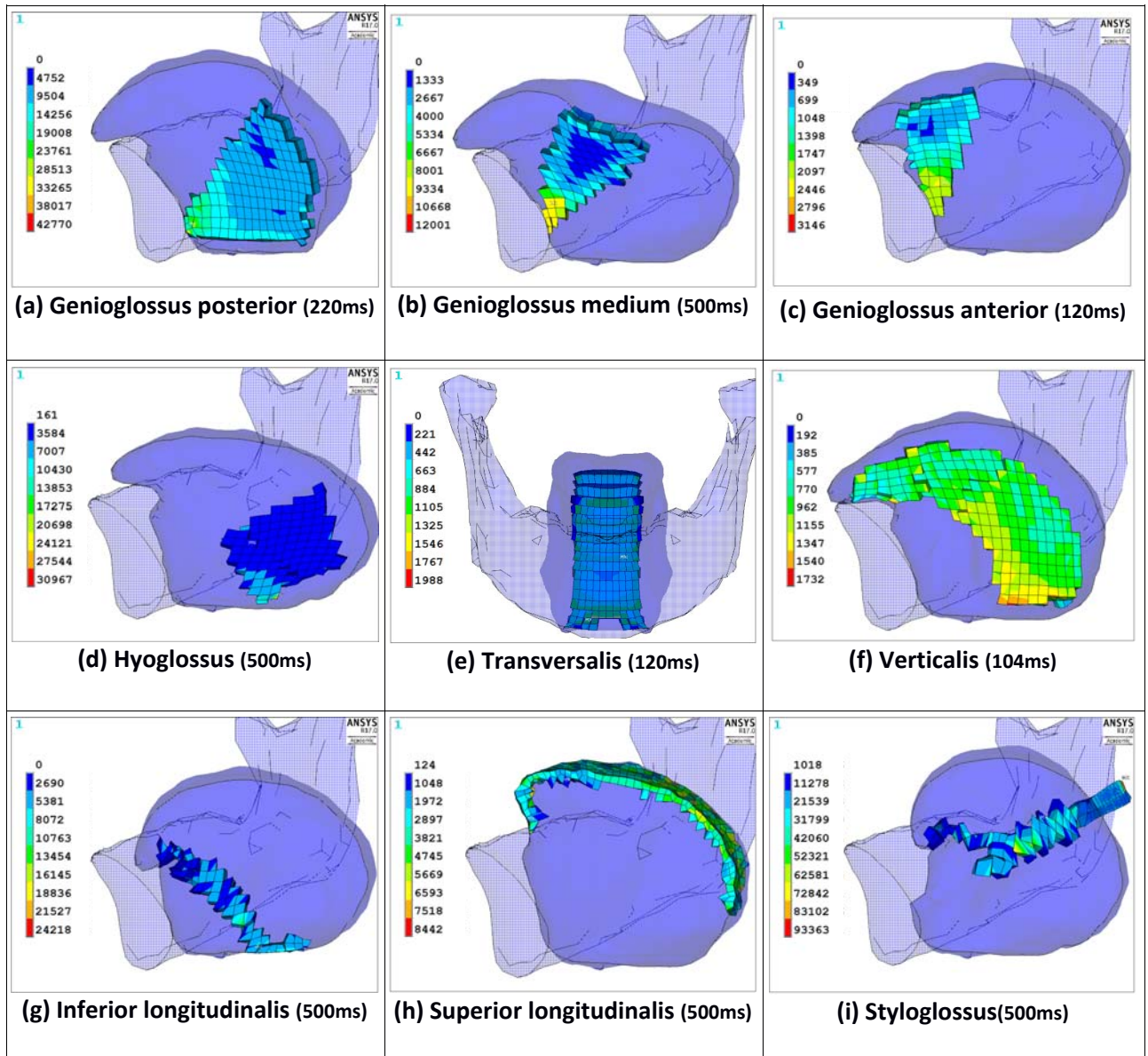


Figure 8: Sagittal cut (except for (e): front view) of mandible and tongue deformed shape due to individual muscle activation (with suitable activation durations – see text). The color scale is used to show the Von Mises Stress values (in Pa). Each muscle is depicted as fully opaque, while the remaining parts of the tongue are partially transparent.

Figure 8 provides the stresses generated in each activated muscle. As expected, important variations in terms of stress amplitudes are observed across muscles, which reveals differences in the level of “resistance” provided by tongue tissues to muscle activation. For example, the anterior part of the Genioglossus muscle can quite easily lower the tongue tip while the posterior part of this muscle needs much more force to bring forwards the large amount of tissues located at the back of the tongue. It is also important to note that the maximum active stress values reported across simulations stay below 100kPa (a maximum value of 90kPa is observed to pull the tongue up towards the soft palate, under the action of the Styloglossus muscle) which is coherent with the 100kPa maximum value proposed by Titze (1994) for the laryngeal muscles and with the 150kPa value suggested by Wang et al. (2013) for tongue muscles.

Finally, it is interesting to discuss the fact that a very soft material was chosen to account for tongue tissues elasticity. Indeed, an equivalent shear modulus μ of 384 Pa was chosen here in agreement with the values reported by Gerard et al., 2005 from ex vivo measurements. This makes the tongue tissues between 3 and 7 times softer than the other material models listed in table 1. To support this choice, we decided to model the way tongue deforms when the subject is laid in a supine position. This is a valuable approach since the supine position is the one of a patient undergoing orofacial surgery, and it is known that in that case, due to anesthesia, the tongue falls backwards and gets in contact with the pharyngeal walls. Indeed, anesthesia suppresses tongue muscles tones and the surgeon has to retain mechanically the tongue in the anterior part of the mouth to make breathing possible for the patient. Two simulations were therefore carried out, both with a gravity direction corresponding to the subject in a supine position. The first simulation (Figure 9, left panel) was done with the current version of the tongue tissue model, while the other one (Figure 9, right panel) assumed a stiffer material, with an equivalent shear modulus μ of 2074 Pa. The current version of the model assumes a purely passive constitutive law while the material chosen for the second simulation was proposed by Buchaillard et al. (2007 and 2009) to account for muscle tone. The results of the simulations are coherent with Buchaillard et al.'s assumptions since our tongue model falls back in contact of pharyngeal tissues (Figure 9, left panel) while taking into account muscle tone prevents the tongue to be in contact with the pharynx (Figure 9, right panel).

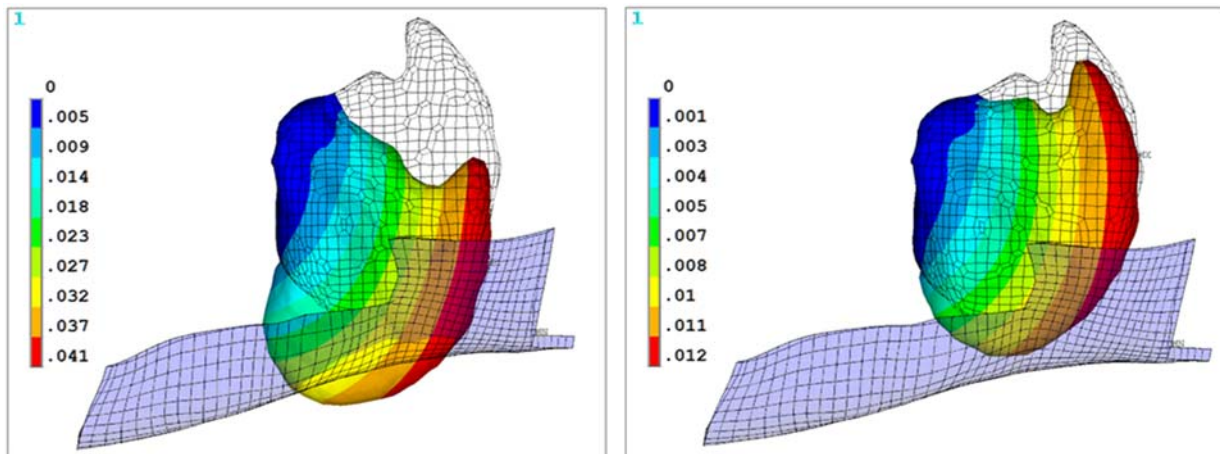


Figure 9: Vertical displacements of the tongue due to gravity for a subject lying in supine position. The two results have been obtained for different C_{10} and C_{20} parameters. Left panel: $C_{10} = 192\text{Pa}$ and $C_{20} = 90\text{Pa}$ (current model); Right panel: $C_{10} = 1037\text{Pa}$ and $C_{20} = 486\text{Pa}$ (from Buchaillard et al. 2007 & 2009).

4. Conclusion

This chapter aims at presenting important issues related to the biomechanical modeling of a complex muscular hydrostat such as the tongue. This organ is characterized by an interweaving of muscular fibers, glands and connective tissues with complex mechanical behaviors. Its shape depends on the recruitment of ten muscles, most of them consisting of independent symmetrical parts with respect to the midsagittal plane. Some of these muscles are internal to the structure, in such a way that, as for the elephant trunk, part of the tongue is responsible for its own deformation.

The mechanical properties of tongue tissues are still not fully captured by the various constitutive models proposed in the literature. In this chapter, the most known computational models assuming a hyperelastic material modeled by using a strain energy approach have been introduced. A focus was given to the works that have proposed a constitutive model inferred from experimental data recorded

either from cadavers or from living subjects' data. Therefore, a Finite Element implementation of an incompressible two-parameter Yeoh strain energy was used to simulate tongue tissues deformations under muscle activations. The corresponding constitutive model was estimated from an indentation experiment done on the fresh cadaver of a 74-year old woman (Gerard et al., 2005).

Results of exhaustive simulations of tongue deformations due to the activations of nine muscles were provided, describing the corresponding displacements, strains and stress fields. It is shown that the very soft material chosen to account for tongue tissues elasticity allowed simulating the very large strains values observed inside the tongue tissues during tagged MRI while maintaining a level of stress in tongue muscles coherent with other data provided in the literature. Such results show the importance of the choice for a constitutive model when the organ model is driven by muscles forces. This is of course not the case when the organ is deformed via imposed displacements (Wittek et al., 2009).

Acknowledgements

This work was supported by a Grant from the “Agence Nationale de la Recherche” (project « Swallowing & Breathing: Modelling and e-Health at Home » (e-SwallHome), Project ID: ANR-13-TECS-0011) and a Grant from Joseph Fourier University and Grenoble-INP (Program AGIR-2013 – Project CLAM).

References

- Barnwell, Y. M., Langdon, H. L., & Klueber, K. (1978). The anatomy of the intrinsic musculature of the tongue in the early human fetus: Part I, M. longitudinalis superior. *The International Journal of Oral Myology*, 4(3), 5-8.
- Bathe, K.-J. (1982). *Finite element Procedures in Engineering Analysis*. Prentice-Hall, Englewood Cliffs, NJ, USA.
- Blemker, S. S., Pinsky, P. M., & Delp, S. L. (2005). A 3-D model of muscle reveals the causes of nonuniform strains in the biceps brachii. *Journal of Biomechanics*, 38, 657–665
- Boë, L.-J., Granat, J., Heim, J.-L., Badin, P., Barbier, G., Captier, G., Serrurier, A., Perrier, P., Kielwasser, N., & Schwartz, J.-L. (2013). Reconstructed fossil vocal tracts and the production of speech. Phylogenetic and ontogenetic considerations. In C. Lefebvre, B. Comrie & H. Cohen (Eds.), *New perspectives on the origins of language* (pp. 75-128), Amsterdam, The Netherlands: John Benjamins Publishing Company.
- Buchallard S., Brix M., Perrier P. & Payan Y. (2007). Simulations of the consequences of tongue surgery on tongue mobility: Implications for speech production in post-surgery conditions. *International Journal of Medical Robotics and Computer Assisted Surgery*, 3(3), 252-261.
- Buchallard S., Perrier P. & Payan Y. (2009). A biomechanical model of cardinal vowel production: Muscle activations and the impact of gravity on tongue positioning. *Journal of Acoustical Society of America*, 126(4), 2033–2051.
- Cheng S., Gandevia S.C., Green M., Sinkus R., Bilston L.E. (2011). Viscoelastic properties of the tongue and soft palate using MR elastography. *Journal of Biomechanics*, 44, 450–454.

- Choi M.G. and Ko H.S. (2005). Modal Warping: Real-Time Simulation of Large Rotational Deformation and Manipulation. *IEEE Trans. Visualization and Computer Graphics*, 11(1), 91-101.
- Dang, J., & Honda, K. (2004). Construction and control of a physiological articulatory model. *The Journal of the Acoustical Society of America*, 115(2), 853-870.
- Feldman, A. G. (1986). Once more on the equilibrium-point hypothesis (λ model) for motor control. *Journal of motor behavior*, 18(1), 17-54.
- Fujita, S., Dang, J., Suzuki, N., & Honda, K. (2007). A computational tongue model and its clinical application. *Oral Science International*, 4(2), 97-109.
- Gefen A. and Margulies S. (2004) Are in vivo and in situ brain tissues mechanically similar? *J. Biomech.*, 37(9), 1339–1352.
- Gerard J.M., Wilhelms-Tricarico R., Perrier P. & Payan Y. (2003). A 3D dynamical biomechanical tongue model to study speech motor control. *Recent Research Developments in Biomechanics*, Transworld Research Network, 1, 49-64. ISBN 81-7895-084-7.
- Gerard J.M., Ohayon J., Luboz V., Perrier P. & Payan Y. (2005). Non linear elastic properties of the lingual and facial tissues assessed by indentation technique. Application to the biomechanics of speech production, *Medical Engineering & Physics*, 27(10), 884-892.
- Gray, H. (1918). *Anatomy of the Human Body*. Philadelphia: Lea & Febiger.
- Hill, A.V. (1938). The heat of shortening and the dynamic constants of muscle. *Proceedings of the Royal Society of London B: Biological Sciences*, 126, 136-195.
- Huxley, A.F. (1957). Muscle structure and theories of contraction. *Progress in Biophysics and Biophysical Chemistry*, 7, 255–318.
- Kahane, J.C., & Folkins, J.W. (1984). *Atlas of Speech and Hearing Anatomy*. Columbus, Ohio: Charles E. Merrill Publishing Company, A Bell & Howell Company.
- Kerdok, Amy E., Ottensmeyer, Mark P., Howe, Robert D., 2006. Effects of perfusion on the viscoelastic characteristics of liver. *J. Biomech.*, 39(12), 2221–2231.
- McMahon, T.A. (1984). *Muscles, reflexes, and locomotion*. Princeton University Press
- Mijailovich S.M., Stojanovic B.,Kojic M.,Liang A., Wedeen Van J. and Gilbert R.J. (2010). Derivation of a finite-element model of lingual deformation during swallowing from the mechanics of mesoscale myofiber tracts obtained by MRI. *J. Appl. Physiol.*, 109, 1500–1514.
- Miyawaki, K. (1974). A study of the musculature of the human tongue. *Annual Bulletin of the Research Institute of Logopedics and Phoniatics*, 8, 23-50.
- Napadow V.J., Chen Q., Wedeen V.J. and Gilgert R.J. (1999). Intramural mechanics of the human tongue in association with physiological deformations, *Journal of Biomechanics*, 32, 1-12.
- Nazari M.A., Perrier P., Chabanas M. & Payan Y. (2011). A 3D Finite Element Muscle Model and its Application in Driving Speech Articulators. *Proceedings of the 23rd Congress of the International Society of Biomechanics, ISB'2011*. Brussels, Belgium.
- Nazari MA, Perrier P, Payan Y. (2013). The distributed lambda (λ) model (DLM): a 3-d, finite-element muscle model based on feldman's λ model; assessment of orofacial gestures. *Journal of speech, language, and hearing research*, 56(6), Suppl., 1909–1923.

- Ottensmeyer, Mark P., 2002. In vivo measurement of solid organ visco-elastic properties. *Stud. Health Technol. Inform.*, 85, 328–333.
- Pelteret JP.V. and Reddy B.D. (2012). Computational model of soft tissues in the human upper airway. *International Journal for Numerical Methods in Biomedical Engineering*, 28, 111–132.
- Rodrigues M.A.F., Gillies D. & Charters P. (2001). A Biomechanical Model of the Upper Airways for Simulating Laryngoscopy. *Computer Methods in Biomechanics and Biomedical Engineering*, 4(2), 127-148.
- Rohan P-Y., Lobos C., Nazari M. A., Perrier P. & Payan Y. (2016). Finite-Element models of the human tongue: a mixed-element mesh approach. *Computer Methods in Biomechanics and Biomedical Engineering: Imaging & Visualization*.
<http://dx.doi.org/10.1080/21681163.2015.1105760>
- Saito, H., & Itoh, I. (2007). The three-dimensional architecture of the human styloglossus especially its posterior muscle bundles. *Annals of Anatomy-Anatomischer Anzeiger*, 189(3), 261-267.
- Schiavone P., Boudou T., Promayon E., Perrier P. & Payan Y. (2008). A light sterilizable pipette device for the in vivo estimation of human soft tissues constitutive laws. *Proceedings of the 30th Annual International Conference of the IEEE Engineering in Medicine and Biology Society, IEEE EMBS 2008*, pp. 4298-4301.
- Simo, J. C., & Taylor, R. L. (1982). Penalty function formulations for incompressible nonlinear elastostatics. *Computer Methods in Applied Mechanics and Engineering*, 35(1), 107-118.
- Stavness I., Lloyd J. and Fels S. (2012). Automatic prediction of tongue muscle activations using a finite element model. *Journal of Biomechanics*, 45, pp. 2841–2848.
- Takano, S., & Honda, K. (2007). An MRI analysis of the extrinsic tongue muscles during vowel production. *Speech communication*, 49(1), 49-58.
- Takemoto, H. (2001). Morphological analyses of the human tongue musculature for three-dimensional modeling. *Journal of Speech, Language, and Hearing Research*, 44(1), 95-107.
- Titze I (1994). Mechanical stress in phonation. *J Voice* 8(2), 99–105.
- Wang Y.K., Nash M.P., Pullan A.J., Kieser J.A. and Röhrle O. (2013). Model-based identification of motion sensor placement for tracking retraction and elongation of the tongue. *Biomech Model Mechanobiol*, 12, 383–399.
- Wilhelms-Tricarico, R. (1995). Physiological modeling of speech production: Methods for modeling soft-tissue articulators, *J. Acoust. Soc. Am.*, 97(5), 3085–3098.
- Wittek A, Hawkins T, Miller K. (2009). On the unimportance of constitutive models in computing brain deformation for image-guided surgery. *Biomechanics and modeling in mechanobiology* Vol. 8(1), 77–84.
- Wu, X., Dang, J., & Stavness, I. (2014). Iterative method to estimate muscle activation with a physiological articulatory model. *Acoustical Science and Technology*, 35(4), 201-212.
- Yang Y., Guo X., Vick J., Torres L.G. and Campbell T.F. (2013). Physics-Based Deformable Tongue Visualization. *IEEE Transactions on Visualization and Computer Graphics*, 19(5), 811-823.
- Zajac, F. E. (1989). Muscle and tendon Properties models scaling and application to biomechanics and motor. *Critical reviews in biomedical engineering*, 17(4), 359-411.

Zemlin, W. R. (1968). *Speech and hearing science: Anatomy and physiology*. Englewood Cliffs, N.J.: Prentice-Hall.